Full Paper

Propellants, Explosives, Pyrotechnics

DOI: 10.1002/prep.201800046

Effects of Dihydroxylammonium 5,5′-Bistetrazole-1,1′-Diolate on the Properties of HTPB Based Composite Solid Propellant

WeiQiang Pang,*[a] JunQiang Li,[a] Ke Wang,[a] XueZhong Fan,[a] Luigi T. De Luca,[b] FuQiang Bi,[a] and Huan Li[a]

Abstract: Several industrial- and research-type hydroxyl-terminated polybutadiene (HTPB) composite solid rocket propellants, containing dihydroxylammonium 5,5′-bistetrazole-1,1′-diolate (TKX-50) particles and, featuring the same nominal composition, were prepared. The energetic properties of composite propellants containing different mass fractions of TKX-50 particles were theoretically computed and experimentally evaluated. The effects of different mass fractions of TKX-50 on the rheological properties of both TKX-50/HTPB binder slurries and AP/HTPB/Al propellant slurries were investigated. The strand burning rates, the associated combustion flame structures, and the hazardous properties of the resulting propellants were experimentally analyzed. All of the properties mentioned above were also compared to those of the reference propellant without TKX-50. The results show that the prepared TKX-50 particles can sufficiently be dispersed in the HTPB binder plasticized by di-2-etylhexyl sebacate (DOS). The propellant compositions containing different mass fractions of TKX-50 are insensitive to impact and friction, differentlyfrom the reference propellant without TKX-50. Moreover, over the explored pressure range, TKX-50 can affect the combustion behavior and decrease the burning rate as well as pressure exponent of composite solid propellants compared with the reference composition.

Keywords: Material chemistry · composite solid propellant · TKX-50 particles · hazardous properties · combustion performance

1 Introduction

High-energy solid propellant compositions play an essential role in propulsion for space exploration. The gravimetric specific impulse and/or density specific impulse of propellants can be increased by the inclusion of certain highly energetic ingredients [1–4]. However, energetic materials (EM) with increased energy content are needed that also have decreased sensitivity toward external stimuli of heating, friction, and impact. In this respect, many efforts are ongoing to design and synthesize new explosives with improved performance. Promising candidates among the new EMs are nitrogen-rich heterocycles. Tetrazole derivatives are among these compounds. In order to improve the energetic properties of the tetrazoles, N-oxides were proposed in several studies as providing even higher densities and stabilities, lower sensitivities and better oxygen balances [5–7]. A new explosive, dihydroxylammonium 5,5′-bistetrazole-1,1′-diolate (TKX-50, chemical structure shows in Figure 1), which belongs to this chemical class, was recently synthesized [8]. According to published data, the explosive performance of TKX-50 exceeds that of RDX and is comparable to that of CL-20. At the same time, it features good thermal stability, low toxicity, and handling safety comparable to that of RDX. It was reported [9–11] that the detonation velocity of TKX-50 (9698 $m \cdot s^{-1}$), calculated at the maximum density of

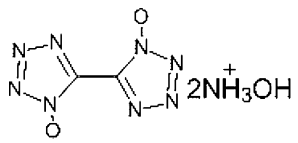

Figure 1. Chemical structure of TKX-50.

1.918 $g \cdot cm^{-3}$ (at 100 K), is higher than that of β-HMX (9221 $m \cdot s^{-1}$) and also of ε-CL-20 (9455 $m \cdot s^{-1}$). At room temperature (298 K), the density of TKX-50 is 1.887 $g \cdot cm^{-3}$. Next to its impressive performance, the impact sensitivity of TKX-50 is 20 J, which is much lower than the sensitivities of RDX, HMX, and CL-20, ranging from 4 to 7.5 J. Friction sensitivity of TKX-50 with 120 N is comparable to or lower than that of RDX, HMX or CL-20. TKX-50 has an electrostatic sensitivity of 0.1 J, which is far higher than what the human body can generate (0.025 J). Finally, the thermal stability of TKX-50

[a] *W.-Q. Pang, J.-Q. Li, K. Wang, X.-Z. Fan, F.-Q Bi, H. Li*
Xi'an Modern Chemistry Research Institute, Xi'an, 710065, P.R.China
**e-mail: Pangwq204@gmail.com*
[b] *L. T. De Luca*
Space Propulsion Laboratory (SPLab), Politecnico di Milano, Milan, I-20156, Italy

with a decomposition onset of 221 °C is comparable to that of RDX.

It is obvious that the highly energetic characteristics of TKX-50 are primarily due to its high enthalpy of formation. Highly energetic performance along with high safety allows considering TKX-50 as not only a powerful explosive [5,12], but also as a promising ingredient for propulsion, which could result in superior propellant compositions. Calculations have shown that TKX-50 is a better replacement of RDX in composite modified double-base (CMDB) propellants [8,9]. Substitution of HMX by TKX-50 in nitrate ester plasticized polyether (NEPE) propellants results in a 2–5 s increase of gravimetric specific impulse. At the same time, neither the combustion behavior nor the combustion mechanism of TKX-50 has been studied up to date. These studies are required for purposeful design and tailoring of TKX-50-based solid rocket propellants.

The properties of any propellant, such as burning rate, pressure sensitivity, etc. are affected by changes in composition (ingredients, and mass fraction), particle size and particle size distribution, and operating conditions (pressure, initial temperature, and so on). There are many different types of propellant ingredients, including oxidizers, binders, and curatives that help to cure the binder, high-energy fillers, metal additives, and catalysts that influence the combustion properties of propellants. The influence of TKX-50 on the properties of composite solid propellants has not been investigated in detail so far. Thus, the purpose of this work is to study the characteristics of the in-house prepared TKX-50 particles, which was synthesis according to the references [7,8] and compare with those of the commonly employed AP by using scanning electron microscope (SEM) and laser granulated analysis diagnostic techniques. Six solid propellant compositions with different mass fractions of TKX-50 particles were produced. The focus of this paper is on how they affect the combustion properties, placing emphasis on the investigation of the hazardous properties, which could be used for solid rocket motor applications.

2 Experimental

2.1 Materials and Specimen

The binder system is composed of hydroxyl-terminated polybutadiene (HTPB, $E_{OH} = 7.8 \times 10^{-4}$ mol/g) plasticized with di-2-etylhexyl sebacate (DOS, $\geq$ 99.4 %), and cured with 2,4-toluene diisocyanate (TDI). Micro-sized aluminum powder, whose mass fraction is 18 % in the composition (Al, d_{50} = 5 μm, purity $\geq$ 99.8 %, purchased from Nanjing Chemical Industry Co., Ltd.) were used as high-energy fuel of the manufactured composite solid rocket propellant. Tri-modal ammonium perchlorate (AP) was utilized in the propellant composition. The first mode consisted of pure research grade (> 99 % pure) AP with an average particle size of 105–147 μm. The second AP mode had an average particle size of 178–250 μm. The third AP mode was made by grinding ammonium perchlorate (> 99 % pure) to an average particle size of around 1–5 μm in a fluid energy mill. TKX-50 particles were well dried before use. Part of the first mode AP mass fraction was replaced by TKX-50 in six propellant compositions, and TKX-50 mass fraction of the samples thus prepared ranges from zero up to 40 % in PHT-1 (0 %), PHT-2 (5 %), PHT-3 (10 %), PHT-4 (20 %), PHT-5 (30 %) and PHT-6 (40 %), respectively. Except where otherwise stated, all propellants were manufactured, processed, and tested at Xi'an Modern Chemistry Research Institute under identical conditions and using identical procedures.

The compositions in terms of ingredient mass fractions of the investigated propellant compositions are shown in Table 1.

Table 1. Main ingredients of composite solid propellant (mass fractions).

Samples	HTPB [%]	Al [%]	AP [%]	TKX-50 [%]	Additives [%]
PHT-1	12	18	68	0	2
PHT-2	12	18	63	5	2
PHT-3	12	18	58	10	2
PHT-4	12	18	48	20	2
PHT-5	12	18	38	30	2
PHT-6	12	18	28	40	2

2.2 Preparation of Propellants

All propellant compositions were mixed in 500 g batches using a vertical planetary mixer of 2 dm^3 capacity. Batches were mixed and cast under vacuum by a slurry cast technique. Propellant was cured at 50 °C for 120 h in a water jacketed oven.

2.3. Characterization Methods of Ingredients and Propellants

2.3.1 SEM and Particle Size Distribution Experiments

Particle size and its distribution were measured by a laser diffraction particle size distribution meter. The morphologies of oxidizers were examined by scanning electron microscopy (SEM). The measured specific surface area values refer to the particle size distribution determined by the Malvern Master Sizer.

2.3.2 Rheological Experiment

The viscosity of the propellant slurry was determined using a HAAKE cylindrical rotational rheometer RS300. The liquid

component of the propellant was mixed with the solid component to form a slurry fluid, the slurry was then mixed with the mixer, with a certain viscosity for the manufacture of the cast propellant. The samples were tested in the co-axial cylinder sensor system at a temperature of about 50 °C.

2.3.3 Burning Rate Test Method

The steady burning rates of propellants were investigated by means of chimney-type linear burner apparatus with observation windows. The measuring apparatus is fully described in Ref. [13]. Propellant samples were placed vertically on the combustion rack of a sealed chamber which was filled with a nitrogen atmosphere. A metal fine wire (0.1 mm in diameter) was threaded through the top of the strand with an alternating voltage of 100 V to ignite the propellant strands (side = 5–6 mm, length = 140 mm) at an initial temperature of 20 °C.

Steady burning rate measurements of propellant samples were performed as follows. When a propellant strand is ignited under the nitrogen gas purge conditions, the pressure in the strand burner increases due to the addition of the gaseous products. However, the pressure valve attached to the nitrogen gas supplier is regulated automatically to reduce the nitrogen gas flow rate in order to maintain the pressure constant. Thus, the pressure in the burner is maintained at the desired pressure. Burning rate is measured by determining the instant of melting of each of 5 low-melting-point fuse wires of lead metal, 0.1 mm in diameter, threaded through the strand at accurately known separation distances. These 5 fuse wires, each in series with a resistor, form 5 parallel arms of an electrical circuit, whose output voltage changes discontinuously as soon as a fuse wire melts. The temperature of the strand is measured by a calibrated copper-constantan thermocouple threaded through the strand with the bead of the thermo couple placed in the center of the strand. Real time data are recorded and processed by a computer which calculates the burning rate. Five experiments are replicated at each test pressure, then the average experimental results are obtained with the standard deviation of 0.13–0.25 [14].

2.3.4 Hazardous Properties Test

The hazardous properties of the tested propellant compositions to impact stimuli were determined by applying the fall hammer method (2 kg drop weight) in a Bruceton staircase apparatus [15] and results are given in terms of statistically obtained 50% probability of explosion (H_{50}). Friction sensitivity was measured on a Julius Peter apparatus [16] by gradually increasing the load from 0.2 to 36 kg, until no ignition was noted in five consecutive test samples.

2.3.5 Heat of Explosion Test

The theoretical heat of explosion was obtained by using "Ideal Gauss Law", It can be calculated according to the equation (1) as follows.

$$H_u = x_1 H_{u1} + x_2 H_{u2} + \ldots x_n H_{un} \quad (1)$$

where H_u is theoretical heat of explosion [$J \cdot g^{-1}$]; x_1 is mass fraction of the first ingredient; H_{u1} is theoretical heat of explosion of the first ingredient [$J \cdot g^{-1}$]; x_2 is mass fraction of the second ingredient; H_{u2} is theoretical heat of explosion of the second ingredient [$J \cdot g^{-1}$]; x_n is mass fraction of the *n-th* ingredient; H_{un} is theoretical heat of explosion the *n-th* ingredient [$J \cdot g^{-1}$].

The measured heat of combustion values can be experimentally verified by means of an isothermal method. A definite mass of propellant sample was put into a calorimetric oxygen bomb, which is surrounded by a fixed mass of water. The propellant was ignited in the bomb and the heat of explosion of the sample was calculated according to equation (2) after the value of the water temperature increase was measured.

$$Q_v = (C\Delta T\text{-}q_1)/m \quad (2)$$

where Q_v is heat of explosion [$J \cdot g^{-1}$]; C is thermal capacity of the calorimeter, J [K]; ΔT is the value of the water temperature increase after the propellant combustion [K]; q_1 is heat of explosion of the initiation wire [J]; m is mass of sample [g].

2.3.6 Density Test

The density measurements were carried out with a Model AG 104 METTLER TOLEDO balance with rectangular shaped samples of 30 mm × 30 mm × 10 mm, which were steeped in a liquid paraffin medium at the temperature of 20 ± 2 °C.

2.3.7 Mechanical Properties

Mechanical characteristics of the tested propellant compositions were determined by an Instron 4505 tensile tester. Cured propellants were cut into slices, from which JANNAF dog-bones were stamped. Tests were carried out at a temperature of 20 °C with 100 mm · min^{-1} cross-head speed.

3 Results and Discussion

3.1 SEM and Grain Size Distribution Analysis

Detailed morphology information concerning the powder was collected by running a series of advanced diagnostic

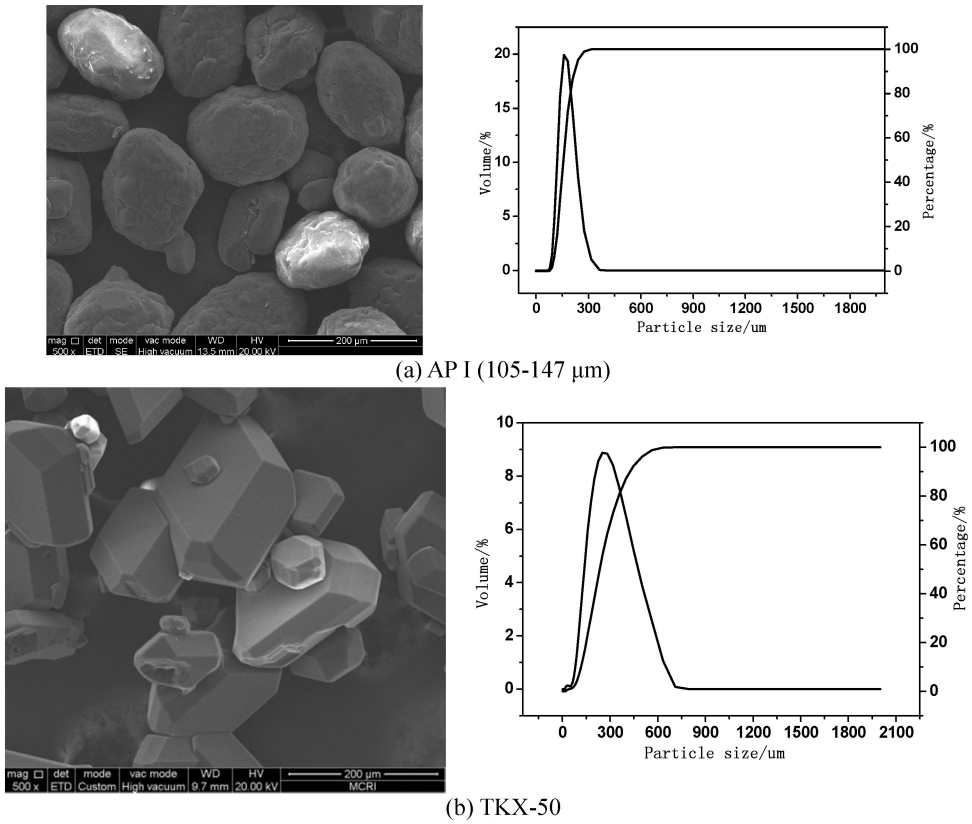

Figure 2. SEM images and grain size distribution of tested particles (× 500).

techniques, including BET, scanning electron microscopy (SEM) and grain size distribution. The well-dried TKX-50 particles were free of fluid, their microstructures and grain size distributions, compared with API (first mode) are shown in Figure 2 and Table 2, respectively.

In the table, width = $(d_{90}–d_{10})/d_{50}$; and specific surface area refers to the particle size distribution determined by Malvern Mastersizer. It should be note that the numbers showed in the table is not much reliable for non-spherical particles.

It can be seen from Figure 2 and Table 2 that the microstructure of the tested TKX-50 particles presents an irregular shape, which are different from those of the near spherical AP used as a reference oxidizer. The d_{50} of TKX-50 particles is 233.7 μm, which is much larger than that of the first mode AP particles and the particle size distribution curve is coarser than that of the common AP. The width of TKX-50 particles is 1.31, which is much higher than that of AP particles (0.686). Corresponding to the higher values of d_{50}, the specific surface area of TKX-50 is 0.03 $m^2 \cdot g^{-1}$, which is much lower than that of AP (1.13 $m^2 \cdot g^{-1}$).

Table 2. Characteristics of AP and TKX-50 particles.

Items	unit	AP (105–147 μm)	TKX-50
d_{10}	μm	111.5	116.9
d_{50}	μm	155.8	233.7
d_{90}	μm	218.4	423.2
Width	–	0.686	1.31
Specific surface area (SSA)	$m^2 \cdot g^{-1}$	1.13	0.03

3.2 Thermo-Chemical and Hazardous Properties of Tested Propellants

3.2.1 Ideal Energetic properties

The energetic properties of composite solid propellants with and without TKX-50 particles were calculated by means of "Energy Calculation Star (ECS)" software [17], which was developed by Xi'an Modern Chemistry Research Institute based on the fundamental thermodynamics principle of minimum free-energy program according to the chemical equilibrium calculation principle. Material density plays an important role in developing high-energy materials. The data obtained are listed in Table 3, and the curve of ideal specific impulse *vs.* TKX-50 mass fractions is shown in Figure 3.

It can be seen that the gravimetric specific impulse (I_{sp}) and characteristic velocity of propellants loaded with TKX-50 particles first increase with an increase in the mass frac-

Table 3. Ideal energetic properties of composite propellants with and without TKX-50 particles (7 MPa).

Samples	I_{sp} [s]	C^* [m s^{-1}]	T_c [K]	$\overline{M}$ [g mol^{-1}]	O [F]
PHT-1	265.4	1589.8	3393.5	26.4	0.527
PHT-2	266.3	1595.2	3333.7	26.6	0.497
PHT-3	266.7	1596.8	3261.4	26.7	0.468
PHT-4	261.4	1573.3	3042.9	25.9	0.413
PHT-5	256.7	1525.5	2698.1	25.5	0.361
PHT-6	255.2	1517.5	2648.2	25.1	0.313

Note: The calculated conditions are as follows: nozzle expansion is 70:1, at atmosphere condition.

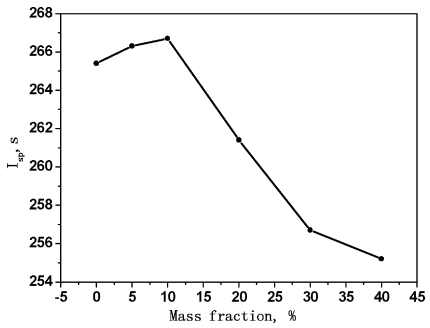

Figure 3. The curve of specific impulse with mass fraction of TKX-50 particles in the propellants.

tion of TKX-50 particles in the compositions and then decrease. The theoretical I_{sp} of propellant is the highest when the mass fraction of TKX-50 is 10%, which may be attribute to the heat of formation of TKX-50 (446.6 kJ·mol^{-1}) is higher and oxygen balance (−27.10%) is lower than that of AP (−290.45 kJ·mol^{-1} and 34.04%), respectively. On the contrary, the adiabatic flame temperature (T_c) decreases with an increase in the mass fraction of TKX-50. The gravimetric specific impulse and characteristic velocity of propellants with differentTKX-50 mass fractions decrease in the following order: [PHT-3] > [PHT-2] > [PHT-1] > [PHT-4] > [PHT-5] > [PHT-6], while the adiabatic flame temperature (T_c) decrease monotonically in the order: [PHT-1] > [PHT-2] > [PHT-3] > [PHT-4] > [PHT-5] > [PHT-6].

3.2.2 Energetic Properties (Density and Heat of Explosion)

Densities and heat of explosion measurements were conducted for each propellant and the results were compared with the theoretical data. Table 4 summarizes the findings of these tests.

It can be seen from the results in Table 4 that the density of composite propellants containingTKX-50 is in the range of 1.734–1.760 g·cm^{-3}, which is lower than that of the propellant without TKX-50 (1.762 g·cm^{-3}). The density of TKX-50 is lower than that of AP, and when parts of AP in the propellant composition are replaced by TKX-50 particles this leads to a decreasing propellant density. Moreover, increasing the high density materials and fine particle percentages leads to an increase in propellant density, which may be due to better powder packing during the manufacturing process. The measured heat of explosion of composite propellant PHT-1 is 6528 J·g^{-1}, which is higher than that of all propellants containingTKX-50 (ranging from 5158 J·g^{-1} to 6441 J·g^{-1}). This may be attributed to the lower heat of formation of TKX-50 (446.6 kJ·mol^{-1}), which results in a lower heat of explosion of the corresponding propellants. Moreover, the values of the measured heat of explosions being lower than that of the theoretical ones, and the heat of explosion efficiency decrease with increase in the mass fraction of TKX-50 in the composition, which may be attributed to the difference combustion efficiency of different mass fractions of TKX-50 powders. However, there is a peak in the heat of explosion efficiency for 10% mass fraction of TKX-50 in the propellant composition. This result agrees with the ideal calculated data. The sequence of the measured heat of explosion and density for the propellants with different TKX-50 mass fractions is the same and is as follows: [PHT-6] < [PHT-5] < [PHT-4] < [PHT-3] < [PHT-2] < [PHT-1].

3.2.3 Hazardous Properties

TKX-50 particles, as one of the most popular high-energy density materials, are very insensitive. Results of the hazardous properties experiments are shown in Table 5.

It can be seen from the results in Table 5 that all the propellant compositions containing TKX-50 were insensitive to impact and friction except the reference one without TKX-

Table 4. Effect of different mass fraction of TKX-50 on the energetic properties for composite solid propellants.

Samples	Heat of explosion [J g^{-1}]		Heat of explosion efficiency [%]	Density [kg m^{-3} ($\times 10^3$)]		Density efficiency [%]
	Theoretical	Measured		Theoretical	Measured	
PHT-1	6609	6528	98.77	1.767	1.762	99.72
PHT-2	6497	6441	99.14	1.764	1.760	99.77
PHT-3	6364	6312	99.18	1.761	1.756	99.72
PHT-4	6026	5838	96.88	1.756	1.750	99.66
PHT-5	5775	5531	95.78	1.750	1.740	99.43
PHT-6	5437	5158	94.87	1.744	1.734	99.42

Table 5. Hazardous properties of composite solid propellants with different mass fraction of TKX-50 particles.

Samples	Friction (*P*) [%]	Confidence level of 95% believe level	Impact [N·m]	Standard deviation S (logarithmic value)
PHT-1	92	(74%, 99%)	4.29	0.04
PHT-2	84	(64%, 96%)	4.71	0.12
PHT-3	80	(59%, 93%)	5.39	0.10
PHT-4	80	(59%, 93%)	11.55	0.11
PHT-5	76	(55%, 91%)	20.05	0.04
PHT-6	72	(51%, 88%)	24.68	0.08

50, which is more sensitive to friction as compared to the other compositions. The insensitiveness may be attributed to the low specific surface area and mechanical insensitivity of TKX-50 particles (impact sensitivity and friction sensitivity is 16% and 24%, respectively) in contrast with AP particles (impact sensitivity and friction sensitivity is 38% and 43%, respectively), especially for ultrafine ammonium perchlorate (UFAP, impact sensitivity and friction sensitivity is 62% and 78%, respectively). The result reveals that the use of the prepared TKX-50 powder in solid propellant leads to a decrease in the sensitivities of friction and impact for the composite solid propellant, making feasible and safe its application in the propellants, whereas, the compositions with different particle size and size distribution of TKX-50 need to be investigated in future.

3.3 Effects of Different Mass Fraction of TKX-50 Particles on the Slurries of Composite solid Propellants

The viscosities of the composite solid propellant with different mass fraction of TKX-50 were determined and the rheological results of the propellant slurry in one hour are shown in Table 6.

Table 6. Effect of different mass fraction of TKX-50 particles on the rheological properties for composite propellants (shear rate: 1 s^{-1}).

Samples	Viscosity [Pa·s]	Yield stress [Pa]	Flowing properties of propellant slurry[a)]
PHT-1	224.4	56.2	A
PHT-2	231.8	58.3	A
PHT-3	254.2	62.4	B
PHT-4	318.8	70.1	B
PHT-5	357.1	79.7	C
PHT-6	389.4	87.2	D

[a)] A-D represents that the flowing properties of a propellant slurry suspension is from good to bad in turn. For the large scale production, the flowing properties of propellant slurry A and B can be acceptable in experimental experience.

It can be found that the rheological properties of the propellant slurry show a behavior of pseudo-plastic, non-Newtonian fluids. TKX-50 particles, when added to the composite solid propellant, increase the viscosity of the slurry insignificantly. The viscosity and yield stress of the reference propellant slurries without TKX-50 (sample PHT-1) were slightly lower than those of propellant slurry containing TKX-50. The characteristics of the viscosity and yield stress for the reference propellant slurries lead to improvement of process properties and pot life [18–20].

3.4 Mechanical Properties of Composite Propellants with and without TKX-50 Particles

Six different series of propellant compositions with and without TKX-50 were tested. The mechanical properties were tested according to the GJB 772A-1997, 413.1 standards and the results are shown in Table 7.

Table 7. The mechanical properties of dual oxidizer composite solid propellants.

Samples	Mechanical properties (+20 °C)		
	σ_m [MPa]	ε_m [%]	E [MPa]
PHT-1	1.08	25.4	6.24
PHT-2	1.10	23.8	6.12
PHT-3	1.14	23.6	5.82
PHT-4	1.19	23.5	5.67
PHT-5	1.29	22.4	5.44
PHT-6	1.34	21.5	5.28

The maximum tensile strength of the referenced composition (1.08 MPa) is lower than those of the propellants containing TKX-50 particles, which is in the range of 1.10–1.34 MPa. Whereas, the elongation and elastic modulus of the referenced propellant (25.4% and 6.24 MPa, respectively) are higher than that of propellants loaded with TKX-50 particles, which are in the range of 21.5%–23.8% and 5.28–6.12 MPa, respectively, which maybe attribute to the addition of irregular morphology and single particle size distribution of TKX-50 particles to the propellant formulation.

In order to analyze the physical structures of composite solid propellants containing different mass fraction of TKX-50, the microstructures of propellants were analyzed, and the results are shown in Figure 4.

Figure 4 can indicate that there are many granulated particles on the surface of cured composite propellants. The prepared TKX-50 particles are compatible with the ingredients of composite solid propellant systems, and the granulated particles with smaller diameters can fill into the spaces between the larger grains sufficiently well.

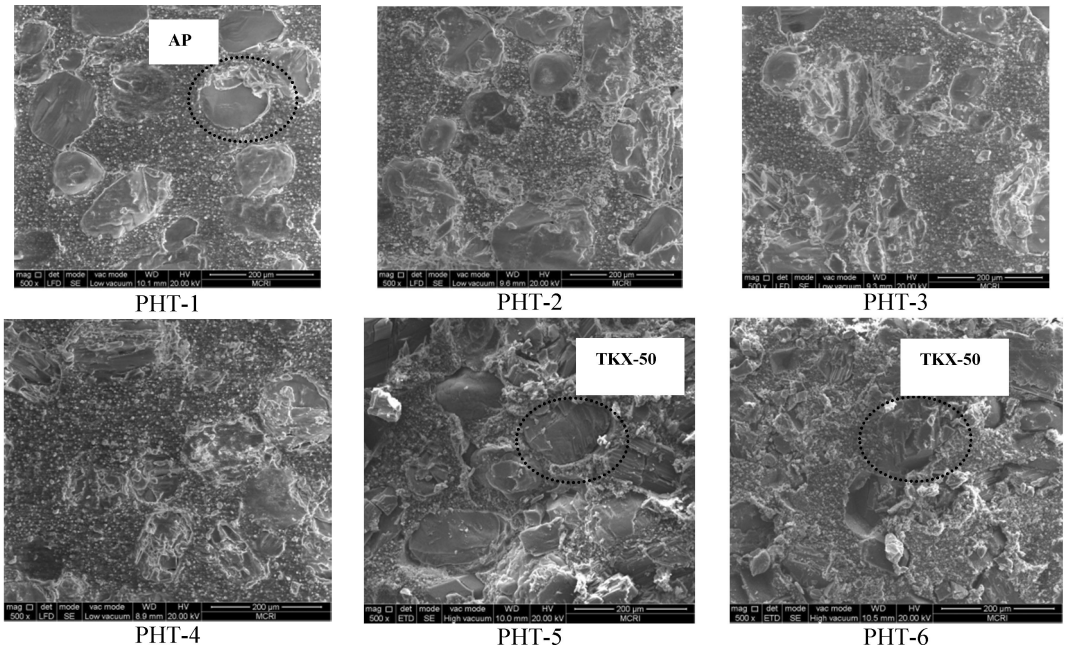

Figure 4. Microstructure surface of composite propellants containing different mass fraction of TKX-50 particles (High magnification (× 500)).

3.5 Effects of TKX-50 Mass Fraction on the Combustion Properties of Composite Propellants

3.5.1 Burning Rate and Pressure Exponent

Propellant burning rates determine the rate of gas generation, which determines the pressure inside the motor and the overall thrust. Burning rates herein are obtained experimentally by burning small propellant strands and measuring the surface regression versus time. Various factors like the particle diameter, oxidizing species, pressure, and temperature may affect the burning rate of propellants. The burning rate data of propellants containing TKX-50 were obtained under different pressures and are shown in Figure 5.

It can be seen in Figure 5 that TKX-50 additives can affect the combustion behavior and change the burning rate of composite solid propellant. The burning rates of all tested samples increase with increasing pressures, and the increasing extent for PHT-6 samples in the pressure range of 1–15 MPa is obviously less than those the other tested samples. The average pressure exponent of PHT-6 sample is 0.245 (1–15 MPa), which is the lowest one among all tested compositions. Moreover, the burning rate and pressure exponent of tested propellant with TKX-50 particles decrease with increasing mass fraction of TKX-50 in the formulation, which may be mainly attribute to the condensed phase combustion phenomena. For the combustion of TKX-50 propellant, the heat feedback from the gas phase maybe cannot provide the necessary heat of release compared with the other high-energy compounds. The addition of TKX-50 in the metalized (μAl) propellant composites prefers to agglomeration would removes a consistent fraction of the combustion energy released in the condensed phase closer to the burning surface and thus sensibly decreases the burning rates [11, 21]. In addition, it is like the onium slats, the decomposition of TKX-50 starts with the equilibrium dissociation of the salt into free acid and base, the surface temperature of onium is controlled by dissociative evaporation, the heat feedback from the gas phase obviously is consumed for evaporation of droplets of un-reacted substance, flowing off the surface. From the view point of heat transfer, the addition of TKX-50 powder to the propellant can decrease the heat adsorption in the combustion process to some extent; from the view of dynamics, TKX-50 powder cannot get in contact with polymer binder and gaseous reactants because of their high insensitivity and relative small specific surface area. Moreover, the releasing heats and heat transmission at the combustion surface for TKX-50 are lower than those of AP at tested pressure range. The increased size of the condensed phase combustion products (CCP) helps in increasing the two-phase flow losses known to be the most serious responsible of performance losses in gas dynamic nozzles, this would be published in the near future.

3.5.2 Thermal Decomposition

In order to analyze the effect of TKX-50 on the combustion mechanism, the thermal decomposition of composite pro-

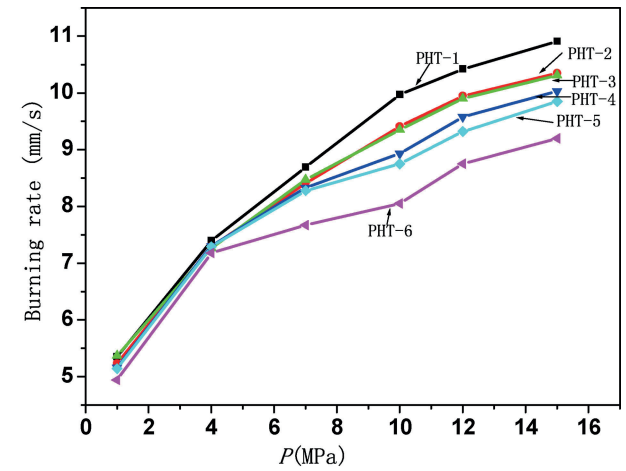

(a) P - r

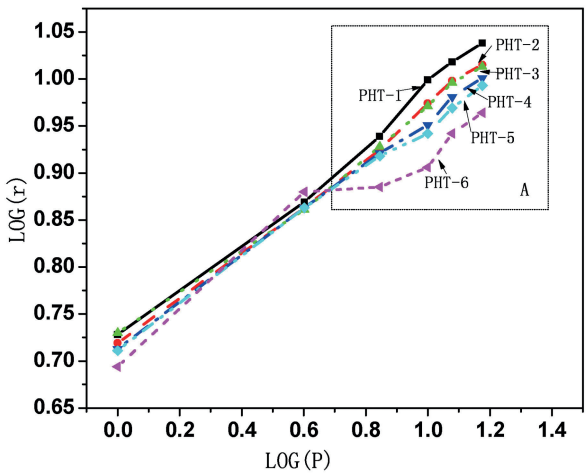

(b) log (P) – log(r)

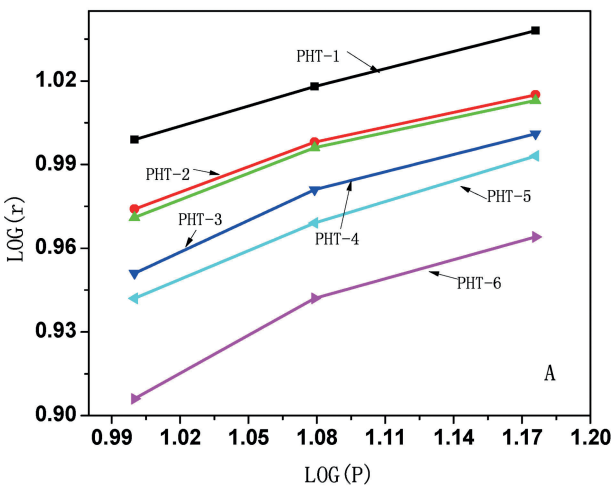

(c) log (P) – log (r)

Figure 5. Burning rate of composite solid propellant containing different mass fractions of TKX-50 particles at various pressures (pressure range: 1–15 MPa; initial temperature: $T_0 = 293$ K). Figure 5 (c) is the enlarged figure of dotted portion in Figure 5 (b).

pellant containing TKX-50 were combined, and the curves shown in Figure 6.

The thermal behavior of TKX-50 and the kinetics of its thermal decomposition were studied using differential scanning calorimetry (DSC) and thermo-gravimetric analysis (TGA) in non-isothermal condition only [22,23], the decomposition mechanism of TKX-50 remains unknown. By applying multiple heating rate of DSC measurements and Ozawa's iso-conversional model free method the activation energy of 135.56 kJ mol^{-1}, and pre-exponential factor of 1.99×10^{12} s^{-1} were calculated from DSC peak maximum temperature *vs.* heating rate relationship [22]. The thermal decomposition of TKX-50 studied by TG-DTA with help of Ozawa's and Kissinger's methods gives close kinetics parameters: 147.32 kJ·mol^{-1} and $10^{12.91}$ s^{-1}, respectively [24]. The apparent activation energy and pre-exponential factor of the exothermic decomposition reaction obtained by DSC measurements and Kissinger's method in Ref. [23] are significantly different: 237.65 kJ·mol^{-1} and $10^{23.89}$ s^{-1}. It can be seen from Figure 6 that the decomposition of composite solid propellants with TKX-50 particles show three exothermic decomposition processes. The first decomposition peak is the main decomposition stage, and there is a little decomposition process affiliated to the first one, the mass loss of thermal decomposition is about 35%, which maybe the decomposition of TKX-50 particles.

4 Conclusions

(1) The TKX-50 prepared particles could be dispersed in the HTPB binder effectively, and their application in the composite propellants, which can be casted in vacuum and cured, is feasible.

(2) The composite propellants containing TKX-50 particles are insensitive to impact and friction compared to the propellant without TKX-50, which is much sensitive to friction as compared to the other compositions.

(3) The TKX-50 particles could be used as the energetic components which would improve the combustion properties of the composite propellant. The addition of TKX-50particles can decrease the burning rates compared to the reference propellant. Also the pressure exponent of the propellants containing TKX-50 particles decrease compared to the reference one (PHT-1 sample).

(4) One must be note that without going into discussion on the calculation methods, we note that the present value of the enthalpy of formation of TKX-50 is highly questionable. It maybe should be investigated further.

Nomenclature

Al	aluminium
AP	ammonium perchlorate
CMDB	composite modified double-base (propellant)

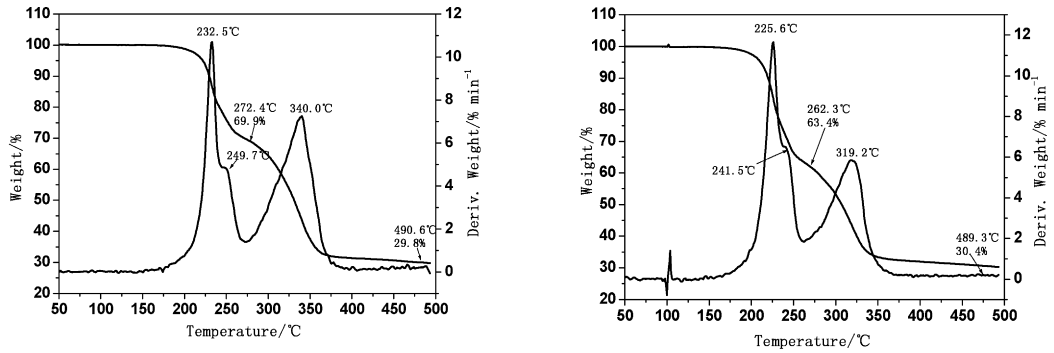

(a) PHT-5 (b) PHT-6

Figure 6. Thermal decomposition of composite propellant containing different mass fraction of TKX-50 particles.

DOS	di-2-etylhexyl sebacate
DSC	differential scanning calorimetry
DTG	differential thermogravimetry
EM	energetic materials
HTPB	hydroxyl-terminated polybutadiene
NEPE	nitrate ester plasticized polyether
SEM	scanning electron microscopy
TDI	2,4 toluene diisocyanate
TG	thermogravimetry
TKX-50	dihydroxylammonium 5,5′-bistetrazole-1,1′-diolate
a	pre-exponential factor of burning rate law
C	thermal capacity of the calorimeter [$J K^{-1}$]
C^*	characteristic velocity [$m \cdot s^{-1}$]
d_{10}	particle diameter corresponding to 10% of the cumulative undersize distribution [μm]
d_{50}	median particle diameter [μm]
d_{90}	particle diameter corresponding to 90% of the cumulative undersize distribution, [μm]
E	elasic modulus [MPa]
E_{OH}	XXX, [$mol g^{-1}$]
ε_m	maximum elongation [%]
H_u	theoretical heat of explosion [$J g^{-1}$]
H_{un}	theoretical heat of explosion of the *n-th* ingredient [$J g^{-1}$]
I_{sp}	gravimetric specific impulse [s]
m	mass of sample [g]
$\overline{M}$	average relative molecular weight [$g mol^{-1}$]
n	pressure exponent
P	pressure [MPa]
ρ	density [$g \cdot cm^{-3}$]
q_1	heat of explosion of the initiation wire [$J g^{-1}$]
Q_v	heat of explosion [$kJ kg^{-1}$]
r	linear burning rate [$mm \cdot s^{-1}$]
σ_m	maximum tensile strength [MPa]
Span	$(d_{90}-d_{10})/d_{50}$
SSA	specific surface area [$m^2 g^{-1}$]
T_c	combustion chamber temperature [K]
x_n	mass fraction of the *n-th* ingredient

Acknowledgement

The authors wish to thank colleagues in the Analyses and Measurements Center, Xi'an Modern Chemistry Research Institute for carrying out scanning electron microscope (SEM), TG-DTG, hazardous properties and combustion structure analyses of the tested experiments and useful suggestions in assessing the statistical data collections.

References

[1] E. W. Price, Combustion of Metallized Propellants, *Fundamentals of Solid Propellants Combustion*, *AIAA Progress in Aeronautics & Astronautics* (Eds.: K. K. Kuo, M. Summerfield), Vol. 90, Chapter 9, Reston, **1984**.

[2] V. A. Babuk, V. A. Vasilyev, V. V. Sviridov, Formation of condensed combustion products at the burning surface of solid rocket propellant, *Solid Propellant Chemistry, Combustion, and Motor Interior Ballistics*, *AIAA Progress in Aeronautics & Astronautics* (Eds.: V. Yang, T. B. Brill, W. Z. Ren), Reston, **2000**, pp. 749–776.

[3] D. Reydellet, *Performance of Rocket Motors with Metallized Propellants* in: AGARD Advisory Report AR-230, AGARD, Paris, France, AGARD PEP WG-17, **1986**.

[4] R. P. Prajakta, V. N. Krishnamurthy, S. J. Satyawati, Differential scanning calorimetric study of HTPB based composite propellants in Presence of nano-ferric oxide, *Propellants Explos. Pyrotech.* **2006**, *31*, 442–446.

[5] A. M. Churakov, V. A. Tartakovsky, Progress in 1,2,3,4-tetrazine chemistry, *Chem. Rev.* **2004**, *104*, 2601–2616.

[6] M. Göbel, K. Karaghiosoff, T. M. Klapötke, D. G. Piercey, J. Stierstorfer, Nitrotetrazolate-1 N-oxides and the strategy of N-oxide introduction, *J. Am. Chem. Soc.* **2010**, *132*, 17216–17226.

[7] F.-Q. Bi, C. Xiao, C. Xu, Z.-X. Ge, B.-Z. Wang, X.-Z. Fan, W. Wang, Synthesis and Properties of Dihydroxylammonium 5,5′-bistetrazole-1,1′-diolate, *Chin. J. Energet. Mater.* **2014**, *22*, 272–273.

[8] V. P. Sinditskii, S. A. Filatov, V. I. Kolesov, K. O. Kapranov, A. F. Asachenko, M. S. Nechaev, V. V. Lunin, N. I. Shshov, Dihydroxylammonium 5,5′-bistetrazole-1,1′-diolate (TKX-50): Physico-Chemical Properties and Mechanism of Thermal Decomposition and Combustion. *2015 International Autumn Seminar on Propellants, Explosives & Pyrotechnics (IASPEP)*, QingDao China, **2015**, pp. 221–238.

[9] N. Fischer, D. Fischer, T. M. Klapötke, D. G. Piercey, J. Stierstorfer, Pushing the limits of energetic materials-the synthesis and characterizationof dihydroxylammonium 5,5′-bistetrazole-1,1′-diolate, *J. Mater. Chem.* **2012**, *22*, 20418–20422.
[10] F.-Q. Bi, X.-Z. Fan, X.-L. Fu, R.-H. Ju, Z.-R. Liu, C. Xu, Interaction of dihydroxylammonium 5,5′-bistetrazole-1,1′-diolate with CMDB propellant components, *J. Solid Rocket Technol.* **2014**, *512*, 214–218.
[11] H. R. Bircher, P. Mäder, J. Mathieu, Properties of CL-20 based high explosives, *29th Int. Annual Conference of ICT*, Karlsruhe, Germany, June 30–July 3, **1998**, paper 94.1-94.14.
[12] L. T. DeLuca, E. Marchesi, M. Spreafico, A. Reina, F. Maggi, L. Rossettini, A. Bandera, G. Colombo, B. M. Kosowski. Agglomeration versus agglomeration in metalized solid rocket propellants, *Int. J. Energetic Mater. Chem. Propuls.* **2010**, *9*, 91–105.
[13] H. F. Huang, Y. M. Shi, J. Yang, Compatibility study of dihydroxylammonium 5,5′-bistetrazole-1,1′-diolate (TKX-50) with some energetic materials and inert materials. *J. Energ. Mater.* **2015**, *33*, 66–72.
[14] N. Fischer, T. M. Klapötke, J. Stierstorfer, C. Wiedemann, 1-Nitratoethyl-5-nitriminotetrazole derivatives- shaping future high explosives, *Polyhedron* **2011**, *30*, 2374–2386.
[15] Z.-S. Zhu, Z.-M. Jiang, P.-C. Wang, M. Lu, Q. Shu, X.-H. Yu, Synthesis and properties of dihydroxylammonium 5,5′-bistetrazole-1,1′-diolate, *Chin. J. Energet. Mater.* **2014**, *22*, 332–336.
[16] J.-F. Wang, Y.-F. Yang, C.-Y. Zhang, X.-J. Wang, X.-P. Zhang, Thermal decomposition reaction kinetics of dihydroxylammonium 5,5′-bistetrazole-1,1′-diolate, *Chin. J. Explos. Propellants* **2015**, *2*.
[17] M. Li, F.-Q. Zhao, Y. Luo, S.-Y. Xu, E.-G. Yao, Energetic characteristics computation of propellants containing dihydroxylammonium 5,5′-bistetrazole-1,1′-diolate (TKX-50), *Chin. J. Energet. Mater.* **2014**, *22*, 286–290.
[18] Q. An, W. G. Liu, W. A. Goddard, T. Cheng, S. V. Zybin, H. Xiao, Initial steps of thermal decomposition of dihydroxylammonium 5,5′-bistetrazole-1,1′-diolate crystals from quantum mechanics, *J. Phys. Chem. C* **2014**, *118*, 27175–27181.
[19] A. E. Fogelzang, V. Yu. Egorshev, V. P. Sinditskii, M. D. Dutov, Combustion of nitroderivatives of azidobenzenes and benzofuroxans, *Combust. Flame* **1991**, *87*, 123–135.
[20] P.-X. Xu, The rheology of polymer and its applications, Chemical Industry Press, Beijing, **2003**.
[21] W.-Q. Pang, X.-Z. Fan, W. Zhang, H.-X. Xu, S.-X. Wu, F.-L. Liu, W.-X. Xie, N. Yan. Effect of Effect of Ammonium Dinitramide (ADN) on the Characteristics of Hydroxyl Terminated Polybutadiene (HTPB) Based Composite Solid Propellant, *J. Chem. Sci. Technol.* **2013**, *2*, 53–60.
[22] G. N. Nazin, G. B. Manelis, Y. I. Rubtsov, V. A. Strumin, Thermal decomposition and combustion of explosives and propellants, CRC Press, Boca Raton, **2003**.
[23] V. P. Sinditskii, V. Yu. Egorshev, V. V. Serushkin, A. I. Levshenkov, M. V. Berezin, S. A. Filatov, Combustion of energetic materials governed by reactions in the condensed phase, *Int. J. Energetic Mater. Chem. Propuls.* **2010**, *9*, 147–192.
[24] V. P. Sinditskii, V. Yu. Egorshev, V. V. Serushkin, A. I. Levshenkov, M. V. Berezin, S. A. Filatov, S. P. Smirnov, Evaluation of decomposition kinetics of energetic materials in the combustion wave, *Thermochim. Acta* **2009**, *496*, 1–12.

Received: February 6, 2018
Revised: August 27, 2018
Published online: October 10, 2018

